Enhanced Release of Small Molecules from Near-Infrared Light Responsive Polymer–Nanorod Composites

Kolin C. Hribar,[†] Myung Han Lee,[‡] Daeyeon Lee,[‡] and Jason A. Burdick[†,*]

[†]Department of Bioengineering and [‡]Department of Chemical and Biomolecular Engineering, University of Pennsylvania, Philadelphia, Pennsylvania 19104, United States

ABSTRACT Stimuli-responsive materials undergo structural changes in response to an external trigger (i.e., pH, heat, or light). This process has been previously used for a range of applications in biomedicine and microdevices and has recently gained considerable attention in controlled drug release. Here, we use a near-infrared (NIR) light responsive polymer–nanorod composite whose glass transition temperature (T_g) is in the range of body temperature to control and enhance the release of a small-molecule drug (<800 Da). In addition to increased temperature and resulting changes in molecule diffusion, the photothermal effect (conversion of NIR light to heat) adjusts the composite above the T_g. Specifically, at normal body temperature ($T < T_g$), the structure is glassy and release is limited, whereas when $T > T_g$, the polymer is rubbery and release is enhanced. We applied this heating system to trigger release of the chemotherapeutic drug doxorubicin from both polymer films and microspheres. Multiple cycles of NIR exposure were performed and demonstrated a triggered and stepwise release behavior. Lastly, we tested the microsphere system *in vitro*, reporting a ~90% reduction in the activity of T6-17 cells when the release of doxorubicin was triggered from microspheres exposed to NIR light. This overall approach can be used with numerous polymer systems to modulate molecule release toward the development of unique and clinically applicable therapies.

KEYWORDS: triggered release · gold nanorods · near-infrared · microspheres · glass transition · responsive

Stimuli-responsive materials have become attractive alternatives to traditional drug carriers due to their ability to control the timed release of their encapsulated contents.[1,2] Polymers that respond to pH,[3−5] light,[2,6,7] and magnetic fields[2,8,9] are just a few examples of the types of materials that have been utilized for triggered drug release. Specifically, near-infrared light (NIR) responsive materials are of particular interest in drug delivery,[2,7,10−13] as NIR light can penetrate body tissue and is minimally absorbed by the body's hemoglobin and water content.[14] Toward this end, gold nanoparticles have the ability to absorb a specific wavelength of light (i.e., NIR) and convert it to heat, called the photothermal effect, making them potential candidates for material heating. Several groups have explored incorporating gold nanoparticles into polymer composites to act as "NIR absorbers,"[15] which allows for heating and resulting drug release.[2,7,10−12,16] Additionally, the photothermal effect has been utilized in cancer irradiation therapy, where cancer cells exposed to gold nanorods and subsequent NIR light were selectively killed *via* photothermal ablation.[17] More recently, other groups have combined photothermal therapy with drug release, demonstrating enhanced, synergistic effects of this combinatorial therapy *versus* either therapy alone.[13,16,18,32]

As an example, the thermoresponsive poly(*N*-isopropylacrylamide) (poly-NIPAAm) has been extensively investigated for triggered drug release.[7,8,19−21,33] Release is primarily controlled by the polymer's lower critical solution temperature (LCST), and when $T <$ LCST, the structure retains a hydrophilic and swollen state; however, when $T >$ LCST, the polymer network becomes hydrophobic and collapses, creating a flux to release its contents. Although poly-NIPAAM gels are effective toward the triggered release of macromolecules, they are not suitable for the delivery of small molecules; such encapsulants passively release from the network in its swollen and nontriggered state ($T <$ LCST),[20] making it difficult to retain them in the absence of a stimulus. Thus, there is still a need for triggered light-responsive systems that can mediate the release of small molecule drugs (*e.g.,* chemotherapeutics).

In this study, we aim to control the release of small molecules *via* the network glass transition temperature (T_g). T_g is a characteristic property that denotes the structural transition from glassy to rubbery states, particularly in highly cross-linked materials, and coincides with a change in the mobility of polymer chains. The tuning

© 2011 American Chemical Society

of a polymer's T_g via copolymerization with hydrophobic monomers and varying network cross-linking density has been successfully used to create clinically applicable products such as self-tying sutures and implantable stents (e.g., through shape-memory relationships); however, this approach has not been investigated for the triggered release of drugs.[22,23] With this in mind, we sought to develop a composite system with triggered release when $T > T_g$ (i.e., rubbery) and, equally as important, to limit passive drug release when $T < T_g$ (i.e., glassy).

In addition to achieving triggered release, the delivery vehicle must also be considered in the context of clinical use. Several groups have explored the use of polymeric discs,[8,24] microparticles,[2,16] and nanostructured materials[1,2,13,16,32] for drug delivery, each of which has its own benefits. Implantable macroscopic discs can offer large reservoirs for drug encapsulation; however, smaller and injectable vehicles such as micro- and nanoparticles have the ability to deliver a higher payload due to their increased surface area to volume ratio.[16] Microspheres of ~40 μm are of interest because they do not migrate into blood and lymph vessels and are not taken up by cells like smaller particles (smaller than 20 μm), nor do they exhibit migration or extensive fibrosis like larger particles (>200 μm).[25]

As a potential example of applicability of this therapy, current chemotherapy involves the intravenous injection of a drug (either free drug or liposomal delivery) and subsequent circulation within the vessels, ultimately accumulating in tumors due to leaky vasculature. However, this process has its limitations, as drug molecules must travel large distances (sometimes >200 μm) from blood vessel to tumor cells while combating a pressure gradient and pH change within the tumor.[26] Additionally, circulation of a small molecule in blood vessels allows for passive uptake in healthy tissue and subsequent immunotoxicity. Thus, the ability to release drug deep in the tissue, as well as remain within the tumor (and prevent entry into healthy tissue), would be beneficial.

Here, we present a polymer−gold nanorod composite that responds to NIR light exposure (LASER ON) to trigger the release of the small-molecule chemotherapeutic drug doxorubicin (MW = 523 Da). In addition, both polymeric discs and microspheres of ~40 μm were investigated as molecule carriers. Upon confirmation of repeatable and triggered release, the therapeutic efficacy of this system was investigated in vitro using cells expressing the cancerous factor HER-2. This work presents a new class of light-triggered polymer−nanorod composites that can provide heating and controlled molecule release.

RESULTS AND DISCUSSION

Polymer Film Formation and Characterization. We previously demonstrated the fabrication of gold nanorod−

polymer composites that exhibit reversible and repeatable heating when exposed to near-infrared light.[15] We illustrated the utility of these composites as shape memory polymers, where shape transitions were triggered by light. In this work, we hypothesized that this same mechanism of transition through the network glass transition temperature (T_g) could be used for alterations in molecule diffusivity through the network for controlled and triggered release.

Polymer films consisting of the degradable poly-(β-amino ester) (PBAE) macromer, A6, and the monomers tert-butyl acrylate (tBA) and 2-hydroxyethyl acrylate (HEA) were formed in the presence of ultraviolet light and the photoinitiator DMPA (0.5 wt %) in a ratio of 10 wt % A6, 20 wt % HEA, and 70 wt % tBA (Figure 1A). PBAEs are a group of biodegradable and cross-linkable polymers whose properties such as T_g can be controlled by the cross-linking density and the hydrophobicity of functional end-groups.[15] The incorporation of the tBA monomer into the A6 network was previously shown to influence network structure and hydrophobicity, and thus viscoelastic properties and degradation (e.g., mass loss of ~5% over 12 weeks) of the resulting network. Specifically, the amount of tBA introduced can be used to tune the T_g to a desired value. In this work, the monomer HEA was also used to increase the solubility of the drug DOX without altering the T_g value. None of these precursors absorb light in the NIR range (Figure 1B). This basic polymer system was used for all studies.

Gold nanorods were synthesized using a seed-mediated growth method.[27] UV−vis spectroscopy reported the characteristic longitudinal (~800 nm) and transversal (~515 nm) absorbance peaks of gold nanorods (Figure 1B). TEM images revealed >90% yield of gold nanorods after synthesis, with an average length, width, and aspect ratio of 31.1 ± 4.5 nm by 9.2 ± 2.8 nm by 3.6 ± 0.8, respectively, with a small fraction existing as gold nanoparticles (squares and spheres in shape). The gold nanorods, originally synthesized in aqueous media, were PEGylated to alter their solubility and transferred to dichloromethane,[28] a step necessary for addition into the largely hydrophobic prepolymer solution. Although the surface plasmon peak shifted slightly during the transfer to organic solvent, it remained well within the near-infrared range (Figure 1B).

Low concentrations of gold nanorods (7.2 × 10^{-13} mol AuNR per gram polymer, ~10^{-8} mass %, ≪1 vol%) were added to the macromer/monomer prepolymer solution (10A6:20HEA:70tBA by wt % with 0.5% DMPA photoinitiator) and photopolymerized under UV light exposure into a film of 1 mm thickness. Dynamic mechanical analysis (DMA) of the polymer film was used to evaluate the storage and loss modulus, and consequently the tan δ, the ratio of loss modulus to storage modulus, over a temperature range. The glass transition temperature was determined to be 40.5 °C
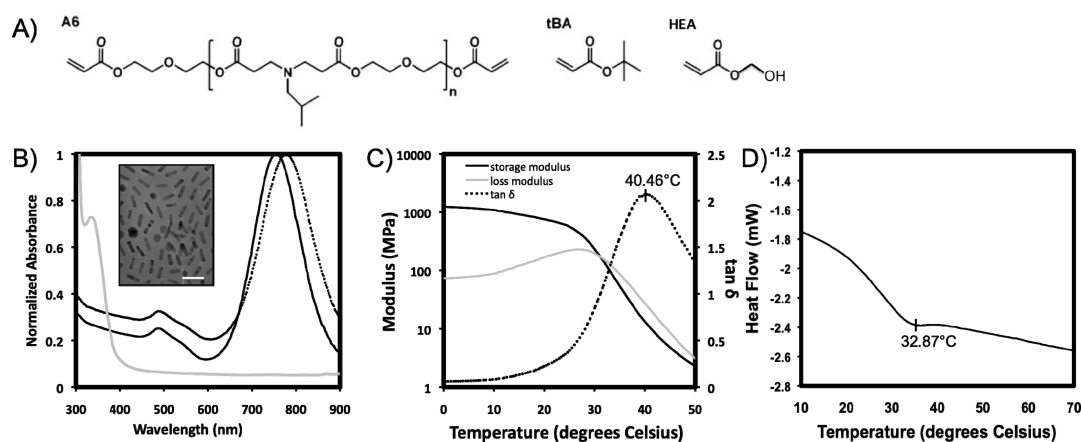
Figure 1. (A) Structures of the macromer A6 (cross-linker, 10 wt %) and monomers tBA (70 wt %) and HEA (20 wt %) used for network formation. (B) Absorption spectra of gold nanorods with original surfactant (black), PEG-modified nanorods in DCM (dotted), and macromer/monomer solution (gray). Inset: TEM image of PEG-modified nanorods (bar = 50 nm). (C) Storage modulus (black), loss modulus (gray), and tan δ (dotted) for 10:20:70 wt % A6:HEA:tBA film containing nanorods tested in tension. The glass transition temperature was determined to be 40.5 °C from the peak of tan δ and 28.5 °C from the onset of a decrease in the storage modulus. (D) DSC of film shows the glass transition temperature to be 32.9 °C, lower than the reported value in (C).

TABLE 1. Properties and Temperatures of Polymer Films and Microspheres Used in Drug Release Studies[a]

material	[polymer] in solution (mg/mL)	nanorod concentration (mol AuNR/g polymer)	$T_{solution}$ (°C)	$T_{polymer}$ (°C)
film	112	7.2×10^{-13}	67.1 ± 2.7	69.9 ± 1.5
microspheres	160	2.16×10^{-12}	49.0 ± 1.5	53.8 ± 1.1

[a] $T_{solution}$ denotes the temperature of the media surrounding the polymer, and $T_{polymer}$ is the surface temperature of the polymer after laser exposure (30 min, 1.1 W).

from the peak of tan δ and 28.5 °C from the onset of a decrease in the storage modulus (Figure 1C). In order to limit passive release of Dox upon incubation at 37 °C, the system was designed to have a T_g near or slightly past body temperature (depending on the technique to assess the T_g value). DSC was used to evaluate the heat flow through the polymer film (Figure 1D). Using this analysis, the T_g was reported to be 32.9 °C, considerably lower than the DMA value calculated from the tan δ peak. The broad temperature range of the glass transition itself can explain this value discrepancy between DMA T_g and DSC T_g. As shown in the DMA results, the transition from glassy to rubbery occurs as the storage and loss moduli decrease, and the decrease extends over a large temperature range. Therefore, the T_g reported in DSC analysis exists within the broad transition range observed with DMA testing. It should also be noted that the addition of nanorods caused a slight (~3 °C) increase in the measured T_g values as reported elsewhere.[15]

Polymer Film Drug Loading and Release. Doxorubicin (DOX, MW = 543), a well-known chemotherapeutic drug that limits cell proliferation by intercalating DNA, was chosen to model the release of small molecules from this polymer system. Its amphiphilic nature
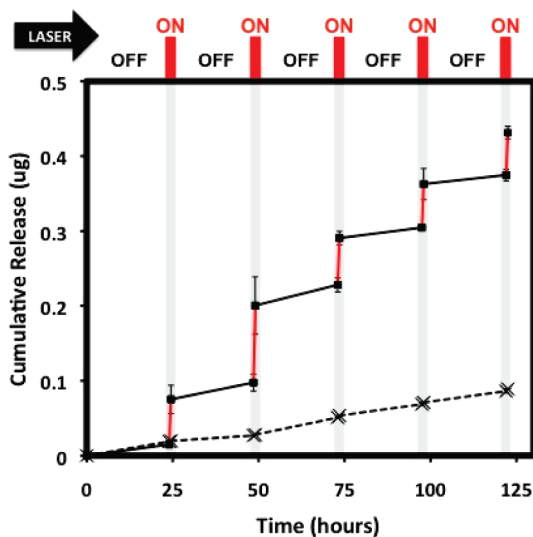

Figure 2. Cumulative DOX release (μg) from polymer discs of two groups: DOX+LASER (—■—) and DOX−LASER (-×-). Five cycles of OFF (24 h, 37 °C) and ON (30 min NIR laser, 1.1 W, red lines) were evaluated. All release studies were performed in triplicate.

and low molecular weight made it ideal for our system, which has both hydrophilic and hydrophobic components. Polymer discs (diameter: 5.8 mm; thickness: 1.0 mm) of ~28 mg in weight were exposed to DOX in methanol (1.0 mg/mL) for 20 min. Subsequent heating at 65 °C was used to remove any solvent from the polymer matrix, leaving the drug encapsulated within. Methanol was the preferred solvent due to DOX's enhanced solubility and the ability to swell the polymer matrix without alteration of any network properties, specifically T_g (~2 °C increase was noted after processing, data not shown). Also, due to the polymer's largely hydrophobic composition, water and other aqueous media were not used in the drug swelling process.
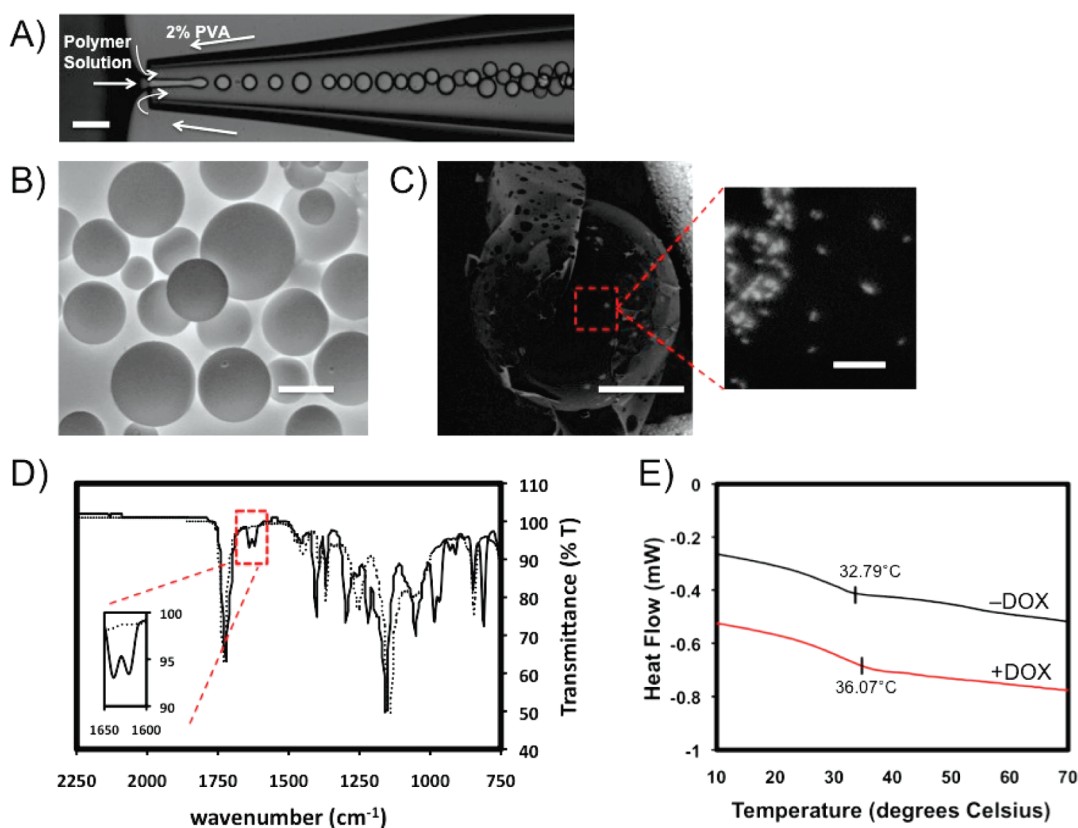
Figure 3. (A) Microspheres were fabricated in a single-emulsion microfluidics device where the outer phase consists of 2% PVA and the inner phase consists of 100% prepolymer solution (bar = 100 μm). (B) Environmental SEM images of microspheres of 10:20:70 A6:HEA:tBA networks after polymerization (bar = 50 μm). (C) Backscattered micrograph image of microspheres containing gold nanorods (bright spots, bar = 20 μm and magnified in image on right (bar = 200 nm)). Perforated folds on the microsphere edge are the flakes of lacey carbon film from the standard TEM grid. (D) FTIR analysis of microspheres before (solid) and after (dotted) polymerization indicating successful double-bond conversion ($\sim$1630 cm^{-1}) with UV light exposure and cross-linking. (E) DSC of microspheres with DOX (red, bottom) and without DOX (black, top). Glass transition temperatures of microspheres without and with DOX were 32.8 and 36.1 °C, respectively.

Upon successful loading of DOX, the polymer discs were washed in PBS and incubated for one week in PBS, to equilibrate the partially hydrophilic matrix with the surrounding aqueous media. Furthermore, any excess DOX was removed from the surface of the polymer during this processing step. At this point, a slight increase ($\sim$4 °C) in the T_g was observed and the actual loading was determined to be $\sim$13.5 μg DOX per disc. The discs (112 mg mL^{-1}, Table 1) were then placed in fresh PBS for the drug release study. To study the LASER ON/OFF release profile of DOX from the polymer–nanorod composite, discs were incubated at 37 °C for 24 h (LASER OFF) followed by NIR laser exposure to the discs for 30 min (LASER ON, Figure 2A). This cycle was repeated five times in order to assess the repeatability and triggered nature of the release. Samples that were exposed to the laser (DOX+LASER) were compared to negative control samples (DOX−LASER) and both groups were normalized to negligible readings for a −DOX+LASER control group.

The average temperature of the polymer discs after 30 min of light exposure in solution was 69.9 °C (Table 1). The LASER ON samples produced a drastic increase in DOX release, while the passive release during LASER OFF was limited. This change in the amount released was repeatable over several cycles, and a $\sim$4.84-fold greater amount of DOX was released with the DOX+LASER group when compared to the DOX−LASER controls (Figure 2). Thus, a stepwise triggered release (DOX+LASER) based on NIR exposure (LASER ON vs LASER OFF) using our polymer–gold nanorod composite system was successfully demonstrated.

Microsphere Fabrication and Characterization. After demonstrating triggered release from our polymer film, we aimed to modify the design of our drug delivery system to create a vehicle that could be implanted via injection (e.g., intratumorally) and activated transdermally with NIR light. Microspheres of $\sim$40 μm in diameter were selected as the ideal drug-delivery vehicle, based on the body's response to materials of various sizes. For example, microspheres of sizes >100 μm were reported to induce a significant macrophage response and fibrosis, whereas particles < 20 μm showed signs of migration and cellular uptake.[25] Microspheres composed of 10 wt % A6, 20 wt % HEA,
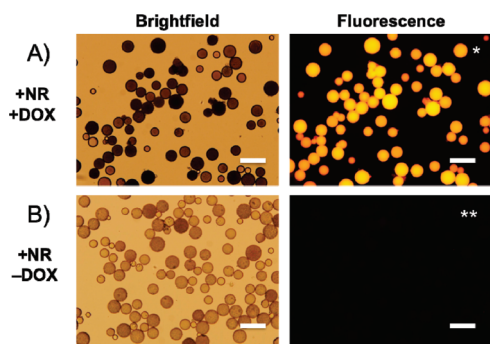
Figure 4. Brightfield and fluorescence images of microspheres consisting of 10:20:70 wt % A6:HEA:tBA with nanorods (bars = 100 μm). (A) Microspheres loaded with DOX (*exposure time = 10.0 ms). (B) Microspheres without DOX (**exposure time = 76.6 ms).

70 wt % tBA (identical composition to the polymer films) with 2.16×10^{-12} mol NR per gram ($\sim 10^{-8}$ mass %, $\ll$ 1 vol%) were fabricated using a custom-built microfluidics device as shown in Figure 3A.[29] An outer aqueous phase composed of 2% PVA solution was pumped into a square capillary tube, flowing around a smaller circular-capillary tube. The organic phase consisting of 100% prepolymer solution flowed from the opposite direction and was flow focused by the aqueous phase, tapering as it reached the circular capillary orifice. As can be seen in Figure 3A, drop formation occurred slightly downstream from the opening of the inner capillary tube, indicating jetting conditions.[29]

This technique produced slightly less monodisperse microspheres than those obtained in the dripping regime[30] (particles formed directly at the opening, not downstream), but was necessary in order to maintain steady microsphere formation. Organic solvents such as dichloromethane were not used in the organic phase due to disruption of the double-bond conversion during photopolymerization of the acrylate functional group, ultimately altering the cross-linking density and T_g of the network.[15] Polymerized microspheres were imaged with SEM (Figure 3B) and backscatter analysis (Figure 3C). A relatively homogeneous distribution, with some clustering, of gold nanorods was observed using backscatter analysis (Figure 3C). Using FTIR, consumption of the peak at $\sim$1630 cm^{-1}, which corresponds to the vinylic double bond of the acrylate group, was observed after photopolymerization (Figure 3D), indicating complete polymerization. Thus, we have developed a process to fabricate nanorod-containing microspheres from liquid precursors.

Microsphere Drug Loading and Release. Microspheres were swelled with a DOX/methanol solution (1 mg mL^{-1}) and rotovapped to remove the methanol solvent. The drug-loaded microspheres reported a 99.7% loading efficiency (of the original 50 μg of DOX swelled into 40 mg of microspheres). DSC was used to determine the T_g of microsphere samples. The T_g values
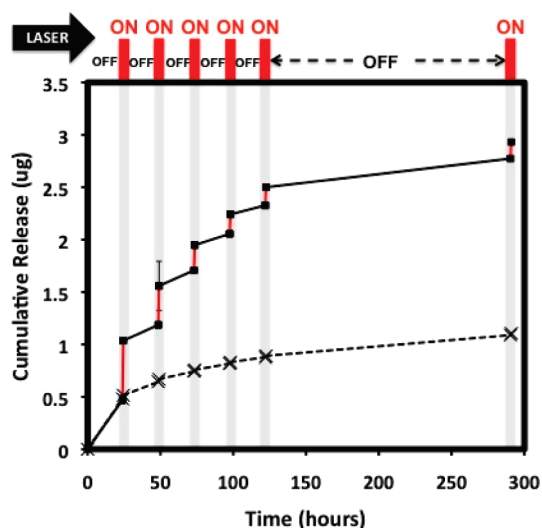
Figure 5. Cumulative DOX release (μg) from microspheres of two groups: MS+DOX+LASER (—■—) and MS+DOX−LASER (-×-). Five cycles of OFF (24 h, 37 °C) and ON (30 min NIR laser, 1.1 W, red lines) were assessed. The sixth cycle consisted of an OFF state (168 h) and ON (30 min NIR laser, 1.1 W). (NOTE: values were normalized to MS−DOX+LASER at the same time points.) All release studies were performed in triplicate.

without and with drug were 32.8 and 36.1 °C, respectively, and were again lower than the expected 40 °C (Figure 3E) but similar to the T_g value reported by DSC for the polymer film (Figure 1D). The increase in T_g is attributed to the processing steps for DOX loading, as a similar change was observed in control samples processed in the same manner, but without DOX (results not shown). As previously described, this lower T_g again can be interpreted as within the broad range of the glass transition. DOX loading was further characterized by imaging drug-loaded microspheres since microspheres containing DOX could be imaged both in brightfield and under fluorescence (Figure 4A), while microspheres without DOX were observed only in brightfield (Figure 4B). The DOX fluorescence imaging demonstrates successful loading of DOX into the microsphere matrix.

Drug release was monitored under the same conditions as the films. The controlled release of DOX from microspheres (160 mg mL^{-1}) with and without laser input for six LASER OFF/LASER ON cycles was evaluated. Microspheres that were exposed to the laser are denoted as DOX+LASER, while the controls (microspheres not exposed to the laser) were denoted DOX−LASER (Figure 5). Each DOX+LASER sample was incubated at 37 °C for 24 h (LASER OFF) followed by NIR laser exposure for 30 min (LASER ON). DOX−LASER samples were incubated at 37 °C for the entirety of the experiment. At each time point, the solution was removed and fresh 2% PVA solution was added to provide sink conditions for the drug release. Cumulative DOX release during six laser cycles is shown in
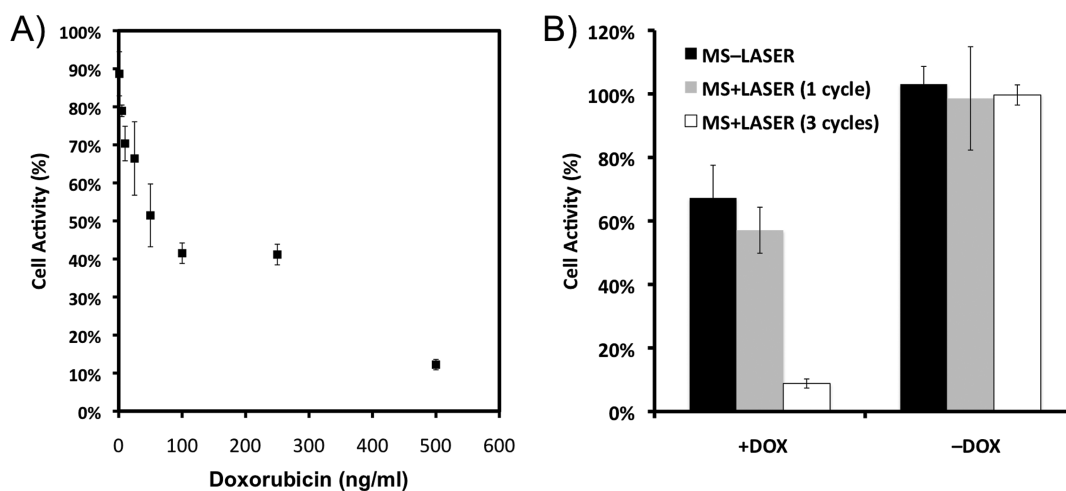
Figure 6. (A) T6-17 cells (5000 cells/well in 96-well plate) were cultured for 24 h in standard media and then another 24 h in media containing various concentrations of DOX (0−500 ng/mL) prior to activity assessment. (B) T6-17 cells (5000 cells/well in 96-well plate, cultured for 24 h) were exposed to 5 mg of MS either with or without encapsulated DOX and either unexposed or exposed for 1 or 3 cycles of 1.1 W NIR light for 5 min with 30 min incubation time between cycles. Cells were cultured for an additional 24 h, and cell activity was assessed. Significant differences in activity were observed between all groups with DOX and all groups without encapsulated DOX, as well as between the group containing DOX with 3 cycles of laser exposure and groups containing DOX with either no laser or only one cycle.

Figure 5A. DOX+LASER samples experienced a 2.7-fold increase in drug release *versus* the DOX−LASER control after six cycles of LASER ON/OFF. Moreover, the drug release occurred in a stepwise fashion (Figure 5), where LASER ON induced a steep increase in drug release, and LASER OFF permitted only a small fraction of drug from being released over a long period. As expected, an initial burst release from the microspheres during the first LASER ON cycle was observed. During the sixth cycle, the samples were incubated in the LASER OFF state for seven days (168 h) at 37 °C followed by a final LASER ON for 30 min.

***In Vitro* Analysis of Microspheres.** T6-17 cells were used to assess cell proliferation/activity in the presence of polymer−nanorod microspheres. T6-17 cells are 3T3 fibroblasts that have been transfected with the growth factor HER-2, commonly overexpressed in breast cancer, and have been previously used in antitumor drug studies involving DOX.[31] As can be seen in Figure 6A, cell proliferation is dose-dependent with respect to DOX; thus, as little as 5.0 ng/mL could inhibit more than 20% cell proliferation, while 500 ng/mL inhibited ∼88% activity.

Microspheres (5 mg) with and without DOX were administered to T6-17 cells in 96-well plates, and each group was subdivided into groups of with and without laser exposure. Cells incubated with microspheres (no DOX) showed 103.1 ± 5.6% cell viability, confirming that the polymer−nanorod microspheres were not toxic themselves to cell proliferation (Figure 6B). MS+LASER (without DOX) confirmed that NIR light exposure and subsequent heating of the microspheres does not affect cell proliferation; after one or three cycles of NIR exposure, MS+LASER samples demonstrated 98.6% or 99.7% cell activity, respectively, which

was not significantly different from MS alone. This is not unexpected since there was essentially no increase in temperature of the culture solution under these conditions (i.e., 37.4 ± 0.8 °C after 1 cycle, 41.0 ± 1.5 °C after 3 cycles).

MS+DOX group (no LASER) demonstrated the passive release nature of the microspheres incubated with cells: these cells demonstrated 67.3 ± 10.3% of cell activity, which was statistically different from all groups not containing DOX. However, DOX-encapsulated microspheres exposed to NIR light (MS+DOX+LASER) demonstrated a varying reduction in cell activity based on the number of NIR cycles performed. Specifically, MS+DOX+LASER samples exposed to one cycle reported 57.1 ± 7.3% cell activity, which was not statistically different from the unexposed and DOX-loaded MS. However, the MS+DOX+LASER samples exposed to three cycles of light showed 8.8 ± 1.4% cell activity, which was statistically different from all other groups. These results demonstrate a heat-activated drug release system whose rate of release and subsequent cell activity can be controlled by exposure time to NIR light. It is also interesting to note that the combination of heat and drug release provides potential synergistic reduction in cell activity, compared to results of either heat or passive drug release alone. This can be attributed to the enhanced drug release during NIR exposure, as confirmed by our previous drug release studies.

CONCLUSION

The work in this study presents a new class of light-triggered responsive composites for controlled drug release based on polymer glass transition temperature. By selecting a glass transition temperature relevant to

the physiological environment, we were able to limit passive diffusion in both films and microspheres, yet release a drug in a repeatable manner with light exposure. Drug-encapsulated microspheres incubated with T6-17 cells and exposed to NIR light exhibited enhanced therapeutic efficacy in terms of limiting cell proliferation. Depending on the application, each system (film or microspheres) was shown to have benefits. For example, polymer films offered large reservoirs for drug encapsulation and also limited passive diffusion, but this was at the expense of a smaller triggered release with light exposure. Microspheres provided a larger cumulative drug release due to their relatively high surface area; however, more drug passively diffused than the film counterpart of the same composition. Further *in vitro* analysis, as well as detailed *in vivo* studies, will be needed to assess this system's applicability for various therapies (*e.g.,* cancer therapy).

METHODS

Polymer and Gold Nanorod Synthesis. Poly(β-amino ester)s were synthesized by the conjugate addition of primary amines to diacrylates by mixing the liquid precursors and reacting overnight (90 °C) with stirring.[15] Specifically, macromer A6 was synthesized through the reaction of diethylene glycol diacrylate (A, Scientific Polymer Products, Inc.) and isobutylamine (6, Sigma) in a 1.2:1 molar ratio. The A6 molecular weight was confirmed to be ~1.3 kDa using ^{1}H NMR spectroscopy (Bruker Advance 360 MHz, Bruker, Billerica, MA).

Gold nanorods were synthesized using a seed-mediated growth method.[27] A seed solution containing hydrochloroauric acid (HAuCl$_4$), cetyltrimethylammonium bromide (CTAB), and sodium borohydride was added to a growth solution of HAuCl$_4$, CTAB, ascorbic acid, and silver nitrate. Gold nanorods formed after several hours. The nanorods' surface was then modified by dropwise addition of mPEG-SH (MW = 5000).[28] Nanorods were transferred to dichloromethane after two rounds of washing and centrifugation (15 min, 16000g) in methanol. The nanorods were imaged on a TEM (JEOL 2010F) at an accelerating voltage of 200 kV by placing a drop of the nanorod/dichloromethane solution on a holey carbon-coated grid (SPI Supplies). Upon imaging, the nanorod dimensions were assessed using ImageJ software. The absorption spectra of the nanorods were also collected (Tecan Infinite M200 UV–vis spectrophotometer).

The photoinitiator 2,2-dimethoxy-2-phenylacetophenone (DMPA, Sigma) was added to a 10:20:70 wt % mixture of the multifunctional macromer A6, the monofunctional hydroxyethylacrylate (HEA), and the monofunctional *tert*-butylacrylate (tBA), respectively, at a final concentration of 0.5% (w/w). The nanorods (in DCM) were added to the monomer/initiator solutions at final concentrations of 7.2×10^{-13} mol per gram of polymer (film) and 2.16×10^{-12} mol per gram polymer (microspheres) (Table 1). The solvent was removed in a vacuum desiccator overnight, and all polymerizations were performed in bulk.

Polymer Film Fabrication and Characterization. Polymer films were produced by injecting the monomer/initiator solution (without and with nanorods) between two glass slides with a 1 mm spacer and polymerizing with exposure to UV light (Blak Ray, ~10mW cm^{-2}, 10 min).[14] The viscoelastic behavior of the samples was determined using a dynamic mechanical analyzer (Q800 TA Instruments). Rectangular strips (25 mm × 5 mm × 1 mm) of polymer were cut from polymer slabs and tested in tension in a controlled strain mode at 1 Hz, an amplitude of 10 μm, and a heating rate of 3 °C min^{-1} from −20 to 80 °C. The T_g is reported as the peak of the tan δ (the storage modulus over the loss modulus) curve and at the onset point of a decrease in the storage modulus.

Polymer Film: Drug Encapsulation and Release. Circular discs (~28 mg, 5.84 mm diameter, 1.0 mm thickness) were cut from polymer films (with and without nanorods). The discs were swelled in 1.0 mg/mL doxorubicin (DOX, in methanol) for 20 min, and the methanol was then evaporated *via* heating at 65 °C for 2 h. The mass swelling ratio (ratio of swollen mass to dry mass) of the discs in methanol was determined to be 2.15 ± 0.04 after the 20 min loading period and 3.79 ± 0.03 after 12 h. Polymer discs were allowed to incubate in PBS (pH 7.4) at 25 °C for five days to ensure that excess DOX was removed, after which the samples were washed quickly in PBS. Reswelling in methanol repeatedly to release entrapped DOX was used to assess total DOX incorporation. DOX release was performed in fresh PBS (250 μL volume for each sample, in square disposable cuvette) for each time point. Samples were exposed to a laser power of 1.1 W (OEM Laser Systems, PL3 808 nm CW laser) for 30 min (LASER ON) and then incubated at 37 °C for 24 h (LASER OFF). PBS from each time point was removed and stored at 4 °C until analysis, and fresh buffer was added. Both the disc surface and solution temperatures were measured with a probe (Microtherma 2T thermometer and MT-D thermocouple probe, Thermoworks) immediately upon removal of the light source. DOX release was determined by fluorescent intensity readings (excitation = 480 nm; emission = 590 nm) using a Tecan Infinite M200 (Männedorf, Switzerland). DOX released from samples (with or without laser, with DOX) was normalized to the experimental control (samples with no DOX, exposed to laser).

Microsphere Fabrication and Characterization. Microspheres were fabricated using a single-emulsion microfluidics device consisting of an inner and outer capillary system.[29] Briefly, the prepolymer solution was delivered (Harvard apparatus, PhD 2000 Infusion) from a syringe (10 mL, SGE Analytical Science) at a rate of 0.5 mL h^{-1} while 2% PVA was delivered in the opposing direction (25 mL syringe, SGE Analytical Science) at a rate of 18 mL h^{-1}. Polymer suspensions budded off at the tip of the inner capillary tube (~100 μm diameter) and remained suspended by the 2% PVA surfactant as they were collected in a glass vial (Figure 3A). Droplet formation was imaged using a Nikon Diaphot 300 with a Nikon TMD/TME automated stage microscope with Vision Research Phantom V7.1 with the accompanying computer software. Microspheres were polymerized in 2% PVA while shaking with exposure to UV light (Blak Ray, ~10 mW cm^{-2}, 10 min). Microspheres were then freeze-dried and stored at room temperature.

The polymerization behavior of microspheres was monitored using attenuated total internal reflectance Fourier transform infrared (ATR-FTIR, Nicolet 6700, Thermo Electron) spectroscopy with a zinc selenide crystal collecting a spectrum every 17 s with a resolution of 3.86 cm^{-1} for 10 min. A small sample of dried microspheres (before and after polymerization) was placed directly on the horizontal crystal, covered with glass, and analyzed. The change in area of the double-bond peak (~1630 cm^{-1}) was used to monitor double-bond conversion with light exposure. Differential scanning calorimetry (DSC) was performed on microspheres (with and without drug) using a Q2000 TA Instruments (New Castle, DE). Samples (~4 mg) were equilibrated at −20 °C and then heated to 80 °C at a rate of 5 °C min^{-1}. As a comparison, DSC was also performed on polymer films. For imaging purposes, microspheres were distributed onto TEM grids with lacey hole carbon film. Microsphere morphology was imaged using environmental scanning electron microscopy, and backscatter micrographs were used to image nanorods within the microspheres by virtue of the microspheres' z-contrast, where higher atomic numbers, z (*i.e.*, gold), appeared as bright spots (Figure 3C).

Microspheres: Drug Encapsulation and Release. A 40 mg amount of dry microspheres was introduced to 50 μL of 1.0 mg mL^{-1} DOX in methanol for 15 min for drug loading. The methanol was then evaporated at 45 °C and 159 mbar using a rotovap (Rotovapor

215, Buchi). DOX fluorescence within the microspheres was examined using an Olympus BX51 fluorescent microscope with TRITC filter. The microspheres were redispersed in 2% PVA, washed three times, and allowed to sit at room temperature for 24 h to remove excess DOX accumulated on the surface. The microspheres were then placed in fresh 2% PVA, and DOX release was measured at various time points (250 μL volume for each sample, in Eppendorf tubes), replacing with fresh 2% PVA each time. A 2% PVA was used for the release solution to prevent microsphere aggregation. Samples were exposed to a laser power of 1.1 W (OEM Laser Systems, PL3 808 nm CW laser) for 30 min for the LASER ON state. For the LASER OFF state (no laser), samples were incubated at 37 °C for 24 h. Reswelling in methanol repeatedly to release entrapped DOX was used to assess total DOX incorporation. DOX release was determined using the same protocol as that of the polymer film (above).

In Vitro Analysis. T6-17 cells (3T3 fibroblast cells transfected with breast cancer HER-2 factor) were plated in 96-well plates (5000 cells/well) in DMEM (10% FBS, 1% penicillin/streptomycin) and allowed to adhere for 24 h. Microspheres with and without DOX were prepared in the same manner as previously mentioned and allowed to incubate in PBS for three days prior to the study to remove excess DOX. The microspheres (MS) were exposed to a germicidal lamp for sterilization and then added to the cells (5 mg/well). Four groups were assessed for cell proliferation: (1) MS; (2) MS+LASER; (3) MS+DOX; (4) MS+DOX+LASER. Cells with MS+LASER and MS+DOX+LASER were exposed to one or three 5 min periods of NIR light (1.1 W, 808 nm) at 30 minute intervals. Cells were cultured for another 24 h, and cell proliferation was assessed with an Alamar Blue assay. Filtered Alamar Blue dye (10% (v/v)) in DMEM media was added to cells and incubated for 4 h. Samples were assessed under fluorescence (excitation: 545 nm, emission: 590 nm) using a Tecan Infinite M200 (Männedorf, Switzerland).

Statistical Analysis. All data are reported as the mean and standard deviation of three samples. For the cellular studies, ANOVA with Tukey's posthoc test was used to determine significant differences ($p < 0.05$).

REFERENCES AND NOTES

1. Stuart, M. A.; Huck, W. T.; Genzer, J.; Muller, M.; Ober, C.; Stamm, M.; Sukhorukov, G. B.; Szleifer, I.; Tsukruk, V. V.; Urban, M.; Winnik, F.; Zauscher, S.; Luzinov, I.; Minko, S. Emerging Applications of Stimuli-Responsive Polymer Materials. *Nat. Mater.* **2010,** *9*, 101–113.

2. Timko, B. P.; Dvir, T.; Kohane, D. S. Remotely Triggerable Drug Delivery Systems. *Adv. Mater.* **2010,** *22*, 4925–4943.

3. Bae, Y.; Nishiyama, N.; Fukushima, S.; Koyama, H.; Yasuhiro, M.; Kataoka, K. Preparation and Biological Characterization of Polymeric Micelle Drug Carriers with Intracellular pH-Triggered Drug Release Property: Tumor Permeability, Controlled Subcellular Drug Distribution, and Enhanced in Vivo Antitumor Efficacy. *Bioconjugate Chem.* **2005,** *16*, 122–130.

4. Ahmed, F.; Pakunlu, R. I.; Srinivas, G.; Brannan, A.; Bates, F.; Klein, M. L.; Minko, T.; Discher, D. E. Shrinkage of a Rapidly Growing Tumor by Drug-Loaded Polymersomes: pH-Triggered Release through Copolymer Degradation. *Mol. Pharmaceutics* **2006,** *3*, 340–350.

5. Prabaharan, M.; Grailer, J. J.; Steeber, D. A.; Gong, S. Stimuli-Responsive Chitosan-Graft-Poly(N-Vinylcaprolactam) as a Promising Material for Controlled Hydrophobic Drug Delivery. *Macromol. Biosci.* **2008,** *8*, 843–851.

6. Katz, J. S.; Burdick, J. A. Light-Responsive Biomaterials: Development and Applications. *Macromol. Biosci.* **2010,** *10*, 339–348.

7. Charati, M. B.; Lee, I.; Hribar, K. C.; Burdick, J. A. Light-Sensitive Polypeptide Hydrogel and Nanorod Composites. *Small* **2010,** *6*, 1608–1611.

8. Hoare, T.; Santamaria, J.; Goya, G. F.; Irusta, S.; Lin, D.; Lau, S.; Padera, R.; Langer, R.; Kohane, D. S. A Magnetically Triggered Composite Membrane for on-Demand Drug Delivery. *Nano Lett.* **2009,** *9*, 3651–3657.

9. Banerjee, S. S.; Chen, D. H. A Multifunctional Magnetic Nanocarrier Bearing Fluorescent Dye for Targeted Drug Delivery by Enhanced Two-Photon Triggered Release. *Nanotechnology* **2009,** *20*, 185103.

10. Wu, G.; Mikhailovsky, A.; Khant, H. A.; Fu, C.; Chiu, W.; Zasadzinski, J. A. Remotely Triggered Liposome Release by near-Infrared Light Absorption Via Hollow Gold Nanoshells. *J. Am. Chem. Soc.* **2008,** *130*, 8175–8177.

11. Wu, W.; Shen, J.; Banerjee, P.; Zhou, S. Core-Shell Hybrid Nanogels for Integration of Optical Temperature-Sensing, Targeted Tumor Cell Imaging, and Combined Chemo-Photothermal Treatment. *Biomaterials* **2010,** *31*, 7555–7566.

12. Kuo, T. R.; Hovhannisyan, V. A.; Chao, Y. C.; Chao, S. L.; Chiang, S. J.; Lin, S. J.; Dong, C. Y.; Chen, C. C. Multiple Release Kinetics of Targeted Drug from Gold Nanorod Embedded Polyelectrolyte Conjugates Induced by near-Infrared Laser Irradiation. *J. Am. Chem. Soc.* **2010,** *132*, 14163–14171.

13. Park, H.; Yang, J.; Lee, J.; Haam, S.; Choi, I. H.; Yoo, K. H. Multifunctional Nanoparticles for Combined Doxorubicin and Photothermal Treatments. *ACS Nano* **2009,** *3*, 2919–2926.

14. Weissleder, R. A Clearer Vision for in Vivo Imaging. *Nat. Biotechnol.* **2001,** *19*, 316–317.

15. Hribar, K. C.; Metter, R. B.; Ifkovits, J. L.; Troxler, T.; Burdick, J. A. Light-Induced Temperature Transitions in Biodegradable Polymer and Nanorod Composites. *Small* **2009,** *5*, 1830–1834.

16. You, J.; Shao, R.; Wei, X.; Gupta, S.; Li, C. Near-Infrared Light Triggers Release of Paclitaxel from Biodegradable Microspheres: Photothermal Effect and Enhanced Antitumor Activity. *Small* **2010,** *6*, 1022–1031.

17. Huang, X.; El-Sayed, I. H.; Qian, W.; El-Sayed, M. A. Cancer Cell Imaging and Photothermal Therapy in the near-Infrared Region by Using Gold Nanorods. *J. Am. Chem. Soc.* **2006,** *128*, 2115–2120.

18. Park, J. H.; von Maltzahn, G.; Xu, M. J.; Fogal, V.; Kotamraju, V. R.; Ruoslahti, E.; Bhatia, S. N.; Sailor, M. J. Cooperative Nanomaterial System to Sensitize, Target, and Treat Tumors. *Proc. Natl. Acad. Sci. U. S. A.* **2010,** *107*, 981–986.

19. Chirra, H. D.; Hilt, J. Z. Nanoscale Characterization of the Equilibrium and Kinetic Response of Hydrogel Structures. *Langmuir* **2010,** *26*, 11249–11257.

20. Bikram, M.; Gobin, A. M.; Whitmire, R. E.; West, J. L. Temperature-Sensitive Hydrogels with SiO_2-Au Nanoshells for Controlled Drug Delivery. *J. Controlled Release* **2007,** *123*, 219–227.

21. Ghugare, S. V.; Mozetic, P.; Paradossi, G. Temperature-Sensitive Poly(Vinyl Alcohol)/Poly(Methacrylate-co-N-Isopropyl Acrylamide) Microgels for Doxorubicin Delivery. *Biomacromolecules* **2009,** *10*, 1589–1596.

22. Lendlein, A.; Kelch, S. Shape-Memory Polymers as Stimuli-Sensitive Implant Materials. *Clin. Hemorheol. Microcirc.* **2005,** *32*, 105–116.

23. Lendlein, A.; Langer, R. Biodegradable, Elastic Shape-Memory Polymers for Potential Biomedical Applications. *Science* **2002,** *296*, 1673–1676.

24. Ortiz, R.; Au, J. L.; Lu, Z.; Gan, Y.; Wientjes, M. G. Biodegradable Intraprostatic Doxorubicin Implants. *AAPS J.* **2007,** *9*, E241–E250.

25. Lemperle, G.; Morhenn, V. B.; Pestonjamasp, V.; Gallo, R. L. Migration Studies and Histology of Injectable Microspheres of Different Sizes in Mice. *Plast. Reconstr. Surg.* **2004,** *113*, 1380–1390.

26. Tredan, O.; Galmarini, C. M.; Patel, K.; Tannock, I. F. Drug Resistance and the Solid Tumor Microenvironment. *J. Natl. Cancer Inst.* **2007,** *99*, 1441–1454.

27. Sau, T. K.; Murphy, C. J. Seeded High Yield Synthesis of Short Au Nanorods in Aqueous Solution. *Langmuir* **2004,** *20*, 6414–6420.

28. Liao, H. W.; Hafner, J. H. Gold Nanorod Bioconjugates. *Chem. Mater.* **2005,** *17*, 4636–4641.

29. Shah, R. K.; Shum, H. C.; Rowat, A. C.; D., L.; J., A. J.; Utada, A. S.; Chiang, L.-Y.; Kim, J. W.; Fernandez-Nieves, A.; J., M. C.; Weitz, D. A. Designer Emulsions Using Microfluidics. *Mater. Today* **2008,** *11*, 18–27.

30. Utada, A. S.; Fernandez-Nieves, A.; Stone, H. A.; Weitz, D. A. Dripping to Jetting Transitions in Coflowing Liquid Streams. *Phys. Rev. Lett.* **2007,** *99*, 094502.

31. Park, B. W.; Zhang, H. T.; Wu, C. J.; Berezov, A.; Zhang, X.; Dua, R.; Wang, Q.; Kao, G.; O'Rourke, D. M.; Greene, M. I.; Murali, R. Rationally Designed Anti-Her2/Neu Peptide Mimetic Disables P185(Her2/Neu) Tyrosine Kinases in Vitro and in Vivo. *Nat. Biotechnol.* **2000,** *18*, 194–198.

32. You, J.; Zhang, G.; Li, C. Exceptionally High Payload of Doxorubicin in Hollow Gold Nanospheres for Near-Infrared Light-Triggered Drug Release. *ACS Nano* **2010,** *4*, 1033–1041.

33. Lee, J. S.; Zhou, W.; Meng, F.; Zhang, D.; Otto, C.; Feijen, J. Thermosensitive Hydrogel-Containing Polymersomes for Controlled Drug Delivery. *J. Controlled Release* **2010,** *146*, 400–408.